3-2-2012

NaBr Poisoning of Au/TiO$_2$ Catalysts: Effects on Kinetics, Poisoning Mechanism, and Estimation of the Number of Catalytic Active Sites

Bert D. Chandler
Trinity University, bchandle@trinity.edu

Shane Kendell
Trinity University

H. Doan

Rachel Korkosz
Trinity University

L. C. Grabow

See next page for additional authors

Follow this and additional works at: https://digitalcommons.trinity.edu/chem_faculty

Part of the Chemistry Commons

Authors

Bert D. Chandler, Shane Kendell, H. Doan, Rachel Korkosz, L. C. Grabow, and Christopher J. Pursell

NaBr Poisoning of Au/TiO$_2$ Catalysts: Effects on Kinetics, Poisoning Mechanism, and Estimation of the Number of Catalytic Active Sites
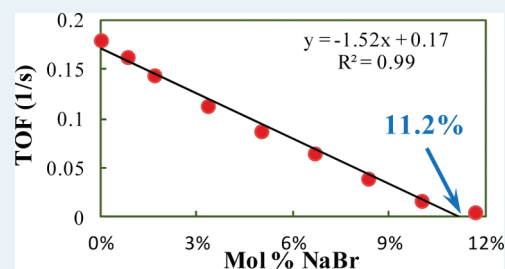
Bert D. Chandler,*,[†] Shane Kendell,[†] Hieu Doan,[‡] Rachel Korkosz,[†] Lars C. Grabow,[‡] and Christopher J. Pursell[†]

[†]Department of Chemistry, Trinity University, San Antonio, Texas 78212-7200, United States

[‡]Department of Chemical and Biomolecular Engineering, University of Houston, Houston, Texas 77204-4004, United States

ABSTRACT: Sodium bromide was used to intentionally poison a commercial Au/TiO$_2$ catalyst with the goals of understanding the nature of halide poisoning and evaluating the number and nature of the catalytic active sites. A series of eight poisoned catalysts were prepared by impregnating the parent catalyst with methanolic solutions of NaBr. Each catalyst was tested with CO oxidation catalysis under differential reactor conditions; O$_2$ reaction orders and Arrhenius activation energies were determined for each material. All of the kinetic data, including a Michaelis−Menten analysis, indicated that the primary effect of adding NaBr was to reduce the number of catalytically active sites. Density functional theory calculations, employed to evaluate likely binding sites for NaBr, showed that NaBr binds more strongly to Au corner and edge atoms than it does to the titania support or to exposed Au face atoms. Infrared spectroscopy of adsorbed CO, along with a Temkin analysis of the data, was also used to evaluate changes to the catalyst upon NaBr deposition. These studies suggested that NaBr addition induces some subtle changes in the coverage dependent properties of CO adsorption, but that these did not substantially impact the CO coverage of the CO binding sites. The experimental and computational results are discussed in terms of possible poisoning mechanisms (site-blocking vs off-site binding and modification); the nature and number of active sites are also discussed in the context of the results.

KEYWORDS: gold catalysts, titania, catalyst poisoning, poisoning mechanisms, halide poisoning, active sites, IR spectroscopy, CO oxidation, Michaelis−Menten kinetics, DFT, Temkin analysis, CO adsorption, electronic effects, coverage dependent adsorption, heat of adsorption

The abstract graphic shows a plot of TOF (1/s) versus Mol % NaBr, with y-axis from 0 to 0.2 and x-axis from 0% to 12%. A linear fit is shown with equation $y = -1.52x + 0.17$, $R^2 = 0.99$, with a data point marked at 11.2%.

■ INTRODUCTION

The high activity of supported gold nanoparticles for catalyzing CO oxidation at sub-ambient temperatures has been well documented over the past 20 years.[1,2] The last several years have seen intense interest in applying Au catalysts to a variety of other reactions[3,4] including the Water-Gas Shift reaction,[5−7] acetylene hydrochlorination,[8] addition of nucleophiles to acetylenes,[9] selective hydrogenation of N−O bonds,[10] alcohol oxidation to acids and aldehydes,[11,12] and direct formation of hydrogen peroxide.[13] In spite of the substantial research activity in gold catalyzed oxidation reactions, the origins of the catalytic activity are still not well understood. Both computational studies and studies on model systems under UHV conditions have shed considerable light onto the unique activity of Au catalysts;[14−16] however, different models suggest a variety of answers to key issues such as the origin of their high activity and the nature of the catalytic active sites.[17] Further, a recent review highlights the difficulties of preparing active supported nanoparticle (NP) catalysts, and the challenges of comparing them to model systems (computational and UHV).[2]

The binding and activation of molecular oxygen is generally considered to be the key catalytic step in highly active Au oxidation catalysts.[2] For CO oxidation, the literature provides a general consensus that O$_2$ activation occurs on only a fraction of the surface Au atoms, probably corner or edge sites.[2] A number of models also propose that O$_2$ is activated at or near the metal−support interface,[1,18] which may partially account for the unusually high sensitivity of Au catalysts to the support material and preparation method. Surface hydroxyl groups may play a role in the catalysis, although it is not clear how actively they participate in the catalytic reaction mechanism.[19] It is now well-known that the preparation of active catalysts requires the complete removal of residual chloride;[1,2,20] consequently, the effects of halide poisoning on Au catalysts is an issue of both fundamental and practical interest.

A continuing fundamental question for Au catalysts, indeed for all catalysts, is the number of active sites. While transmission electron microscopy (TEM) can provide information on particle size, and an estimate of the fraction of surface atoms, it does not directly probe the number of reactive centers on a catalyst surface. Chemisorption experiments provide a measure of the number of reactive centers on a catalyst surface, which may or may not correlate to the number of catalytic active sites. An alternate method for evaluating the number of active sites

on a catalyst is through intentional poisoning experiments. In these experiments, controlled amounts of poison are added to a catalyst and the reduction in activity is monitored. Changes in the catalytic activity as a function of the amount of added poison can therefore shed light onto both the number of active sites and any distribution in the inherent reactivities of the active sites.

Several research groups have applied these techniques. Using ethylene hydrogenation as a probe reaction, Turkevich and co-workers developed a pulse poison/titration experiment with a variety of poisons for supported Pt catalysts in the 1970s.[21] More recently, Finke and co-workers used CS_2 poisoning experiments to evaluate the number of active surface atoms in a 5% Rh/Al_2O_3 catalyst.[22] Applying the same methodology to soluble polyoxoanion stabilized Rh nanoparticles of comparable size allowed the researchers to more precisely compare the inherent reactivities of the two catalysts on a per active site basis. Buriak and co-workers also used CS_2 poisoning to qualitatively compare the number of active sites between monometallic Rh and bimetallic Pt−Rh hydrogenation catalysts.[23] The Kung group also recently studied NaBr poisoning of Au/TiO_2 catalysts with overall activity measurements and a variety of X-ray absorption techniques.[24] That study did not include the detailed kinetics, IR spectroscopy, or computational experiments presented in the current study.

Beyond these examples, similar poisoning studies have not been widely applied in the heterogeneous catalysis literature. Herein, we report a full NaBr poisoning study that adds a detailed kinetic analysis of all the poisoned catalysts. The reaction kinetics studies are coupled with density functional theory (DFT) calculations and infrared spectroscopy of adsorbed CO studies. This study follows the recent study from the Kung group,[24] adding detailed kinetics, IR spectroscopy, and DFT calculations to interrogate the Au/TiO_2 system. In combination, these studies serve as sensitive probes for electronic changes to the catalyst surface, provide substantial insight into the nature of halide poisoning for these materials, and shed light onto the number and nature of CO oxidation active sites.

■ EXPERIMENTAL SECTION

Materials and Reagents. Water was purified to a resistivity of 17−18 MΩ-cm with a Barnstead Nanopure system. All gases were Praxair 5.0 grade cylinders and used without further purification. The 5% CO/He mixture was purchased in an aluminum cylinder to avoid potential contamination by iron carbonyls. The Auricat test catalyst (ATC) (Au/TiO_2) was purchased from Strem and stored in the dark in a refrigerator. NaBr was purchased from Fisher Scientific and methanol from Aldrich.

Addition of NaBr. Methanolic solutions of NaBr were prepared with concentrations such that incipient wetness impregnation of the catalyst yielded the desired Br^-:Au ratio. A typical impregnation consisted of the following: from a 1.45 mmol L^{-1} NaBr solution, 70.0 μL was pipetted by a mechanical pipetor (VWR) and added to 100 mg of Au/TiO_2 catalyst. The resulting slurry was stirred thoroughly to ensure uniform distribution. The impregnated catalyst was dried at room temperature in a fume hood for 1 h, then at 135 °C for 24 h. The solid was then ground to a fine powder for catalytic testing. This preparation yielded a poisoned catalyst with a Br^-:Au molar ratio of 1.7%. By varying NaBr concentration of the impregnating solution, a total of eight poisoned catalysts

(Br^-:Au = 0.8%, 1.7%, 3.3%, 5.0%, 6.7%, 8.3%, 10%, and 12%) were prepared. Each catalyst was prepared twice; reported catalysis results are for two different preparations.

Elemental Analysis via Inductively Coupled Plasma-Optical Emission Spectroscopy (ICP-OES). The Au content was determined using a Varian 720-ES, ICP Optical Emission Spectrometer. Approximately 300 mg of catalyst was accurately weighed in a beaker. Freshly prepared aqua regia (6 mL) was then added to the sample and allowed to digest at room temperature for 30 min. The sample was then heated slowly to 60 °C for 2 h, and the resulting solution was filtered into a 25 mL volumetric flask. The sample was diluted to mark with nanopure water and subsequently analyzed. The gold concentration of the solution was determined to be 148 ppm, indicating a 1.2% Au loading for Au/TiO_2. Experimental errors for the method and the spectrometer are typically less than 5%, and the result was in excellent agreement with previous determinations using atomic absorption spectroscopy.[25]

CO Oxidation Catalysis. The CO oxidation reactor system consisted of a previously described home-built laboratory scale single pass plug-flow microreactor.[25] Feed and catalyst effluent CO, CO_2, and O_2 compositions were determined using Siemens Ultramat 23 infrared gas analyzer. Supported catalyst samples (3 to 10 mg based on degree of poisoning) were diluted with approximately 1 g of 400 mesh silicon carbide (Aldrich) and placed in the microreactor. All reactions were performed at ambient pressure with 1% CO in the feed, which was maintained with Porter mass flow controllers. Catalysts were pretreated with 10%H_2-10%O_2-80%N_2 (120 mL min^{-1}) for an hour at 250 °C. After pretreatment, the furnace was removed, and the catalyst was allowed to equilibrate under flowing 1% CO + 20% O_2 (180 mL/min) for 1 h. An ice and/or water bath was then placed around the catalyst to control the reaction temperature. Changes in CO oxidation activity were measured as a function of temperature as well as CO and O_2 feed concentration. All activities were determined by averaging steady state conversion data for approximately 10 min, usually between 1 and 3 h after introducing CO to the activated catalyst. Each activity measurement was performed with a fresh catalyst sample.

Infrared Spectroscopy of Adsorbed CO. Infrared spectroscopy experiments were performed as previously reported.[26,27] Approximately 25 mg of the Au/TiO_2 catalyst was pressed into a 30 × 30 Ti mesh (Unique Wire Weaving Co.). The resulting mesh-supported pellet was placed in a tube furnace and heated overnight at 135 °C. After cooling, the mesh-supported pellet was mounted into a home-built copper cell and vacuum chamber with a gas-phase optical path length of 1 cm. The entire vacuum chamber was placed in the sample compartment of a Nicolet Magna 550 FTIR spectrometer and evacuated to a pressure of <1 mTorr for 15 min. All measurements were made at 273 K, and all spectra were referenced to a background spectrum of the catalyst pellet under vacuum prior to the addition of CO. Transmission spectra consisted of 100 scans collected with 8 cm^{-1} resolution (spectral data spacing = 4 cm^{-1}) and were reported in absorbance units.

The gas handling system consisted of a mechanical and diffusion pump, a glass line with stainless steel transfer lines to the sample apparatus, and a Baratron pressure gauge (P = 0 to 20 Torr). A liquid nitrogen trap was used to trap out any impurities from the CO tank (UHP grade, from Air Products). The entire gas handling system was rinsed with CO three times

before exposing the sample. After collecting a background spectrum, the sample was exposed to a low pressure of CO, and the surface was allowed to equilibrate for 5−10 min; previous work has shown that this is ample time for CO equilibration on Au catalysts.[26,27] An infrared spectrum was recorded, and the pressure in the cell was slowly increased to the next pressure. After completing an experiment, the sample was evacuated and the experiment repeated for a total of two or three adsorption isotherm measurements on a single catalyst sample in a single day.

Computational Methods. All calculations were performed using the grid-based projector augmented wave DFT code GPAW[28,29] and the Atomic Simulation Environment (ASE).[30] Electron densities and wave functions were represented on real-space grids with a grid spacing of 0.18 Å in all directions of the unit cell. The revised Perdew−Burke−Ernzerhof (GGA-RPBE) functional[31] was used to describe exchange and correlation, and the Brillouin zone was sampled using a 4 × 4 × 1 Monkhorst-Pack k-point set.[32] The Kohn−Sham states were populated using a Fermi−Dirac distribution with $k_bT = 0.1$ eV, and total energies were then extrapolated to $k_bT = 0$ eV. Gold surfaces were modeled as slabs with a (2 × 2) unit cell for the closed-packed fcc(111), a (2 × 1) unit cell for the stepped fcc(211), and a (1 × 1) unit cell for the kinked fcc(532) surface. The theoretically obtained lattice constant of 4.222 Å was used for all calculations. Slabs were separated with a vacuum of 12 Å along the normal direction of the surface. The fcc(111) surface was modeled as four-layer slab where the top two layers were allowed to relax, while the bottom two layers were fixed in their bulk positions. The slabs for the fcc(211) and fcc(532) surfaces were modeled with an equivalent thickness and constraints with the fcc(111) surface. The binding energy E_b was calculated using the following equation:

$$E_b = E_{ads+slab} - E_{slab} - E_{gas} \qquad (1)$$

where E_{slab} is the energy of the slab, E_{gas} is gas phase reference energy of the adsorbed species, that is, CO, O, Br_2, NaBr, and $E_{ads+slab}$ is the total energy of the slab with adsorbate.

■ RESULTS

Catalyst Pretreatment and Evaluation of Reaction Conditions. Initial experiments were performed on the 1% Au/TiO$_2$ catalyst to identify catalyst activation conditions that optimized and balanced catalytic activity and selectivity. Treatment with O$_2$ followed by H$_2$ at 300 °C yielded materials with good catalytic activity, but the catalyst rapidly deactivated, losing more than 50% of its initial activity in an hour. Pretreating the catalyst with a mixture of oxygen and hydrogen considerably enhanced stability. On the basis of numerous experiments varying the feed composition and pretreatment temperature, we found a pretreatment of 10% O$_2$-10% H$_2$-80% N$_2$ at 250 °C for 1 h to be optimal.[25] After pretreatment, catalysts were cooled to room temperature under flowing N$_2$ and a feed of 1% CO/20% O$_2$ balance N$_2$ was introduced.

The catalyst was typically very active following the pretreatment. This initial high activity decreased rapidly and stabilized over the course of 30 min to 1 h at room temperature. After 1 h, an ice/water bath was placed around the U-tube reactor. Stability tests at 0 °C showed that the catalytic activity measurement varied by ±5% over 2.5 h and that any deactivation was within this inherent measurement error.[25]

Because of the difficulties associated with maintaining the very low conversions (<5%) used in our previous studies with Au/TiO$_2$ catalysts,[25,33] flow rate was varied from 60 to 180 mL/min under a reaction atmosphere of 1% CO−20% O$_2$ (balance N$_2$). Figure 1 shows that CO conversion was linear
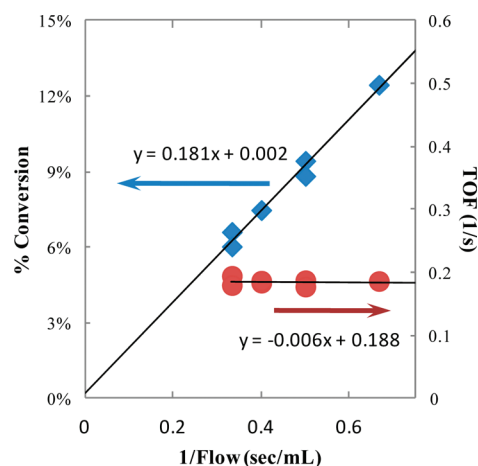

Figure 1. % Conversion and TOF vs 1/Flow during CO oxidation catalysis over 1% Au/TiO$_2$.

with the inverse space velocity (1/Flow, or residence time) for conversions of up to 13%. Turnover frequencies measured at these conditions are therefore independent of flow rate, and were calculated directly from the conversion data. It is also worth noting that deviations from this linear region begin at 17% conversion. Therefore, all subsequent catalysis studies were performed with CO conversions below 12%. Typically, conversions of 5−10% were used as this provided somewhat better precision in the measurements.

Catalytic Activity of Bromide Poisoned Catalysts. The primary goals of this study were to increase our understanding of the nature of halide poisoning on Au catalysts and to examine intentional bromide poisoning as a potential method for evaluating the number of active sites on Au catalysts. Bromide was added to the catalyst via incipient wetness impregnation using a methanolic solution of sodium bromide. Previous work by the Kungs' group has shown that such impregnations result in sodium bromide associated primarily with the Au nanoparticles.[24] For comparing the overall activity of the poisoned materials, CO oxidation catalysis was performed with initial conditions of 1% CO and 20% O$_2$.

Arrhenius studies (Figure 2) show that NaBr addition decreases catalytic activity; however, the apparent activation energy appears to be relatively unaffected by NaBr. Figure 3 presents systematic poisoning (18 independent experiments) of the Au/TiO$_2$ catalyst with NaBr. The data show a linear decrease in CO oxidation activity with added NaBr; note that the x-axis is the mole % of NaBr relative to the total amount of Au in the catalyst. The x-intercept in Figure 3, which indicates the amount of NaBr required to eliminate all of the catalytic activity, is 11.2%. In other words, 11.2 mol % NaBr, relative to total Au, is sufficient to completely poison the catalyst. This is in good general agreement with a similar study from the Kungs' group.[24] TEM data on this catalyst show the mean particle diameter to be 3.2 nm,[25] meaning that roughly 35−40% of the Au atoms are on the surface of the nanoparticles.[34] Thus, the x-intercept in Figure 3 corresponds to approximately 30% of the surface Au atoms (cf. 37% (fraction of surface Au) × 30% ≈
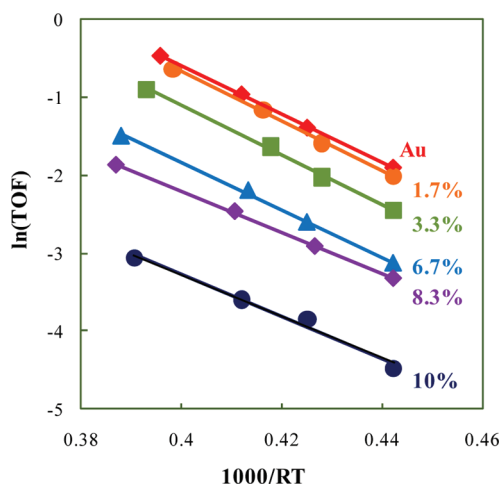
Figure 2. Arrhenius plots for Au and 5 NaBr poisoned catalysts, showing negligible change in apparent activation energy. NaBr mole percents (relative to total Au in the catalyst) are indicated to the right of each data set.
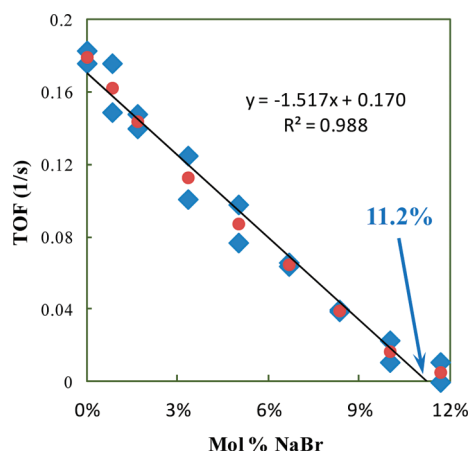

Figure 3. CO oxidation activity as a function of added NaBr at 0 °C. Data show two separate runs for each catalyst; the average is plotted in red circles.

Figure 4. Catalyst deactivation with time and oxygen reaction order correction for the 8.3% NaBr catalyst. The solid blue circles show the raw data with the relative time (in minutes) listed next to each point. Open green diamonds show the corrected data, setting the first and last point to the same TOF.

Figure 5. Oxygen reaction order data for NaBr poisoned Au/TiO_2 catalysts. Data were corrected for any deactivation as shown in Figure 4 and described in the text. NaBr mole percents (relative to total Au in the catalyst) are indicated to the right of each data set.

11% total Au). In other words, the catalytic activity is essentially gone when one NaBr has been added for every 4 surface Au atoms.

As might be expected, the poisoned catalysts were more susceptible to deactivation over time than the unpoisoned catalyst. This complicated O_2 reaction order studies, because even moderate deactivation (10% over 2 h) causes a systematic error in the determined reaction order. An example of this systematic error can be found in Figure 4, which shows data for the 8.3% NaBr catalyst, where the catalyst deactivates by 10% of the initial activity over about 2 h. The raw data is shown with the relative time of the data collection next to each data point. Since data was collected from high pressure to low, the successively lower activities over time cause the observed reaction order to be artificially large (note that the slope of blue points in Figure 4 is substantially larger than the slope of the corrected data). The data was therefore corrected for deactivation by calculating the rate of deactivation between the first point (20% O_2, filled circles in Figure 4) and the fifth point (20% O_2). Points in between were then corrected assuming that the deactivation was linear over this time. The corrected TOF values were subsequently used to determine the
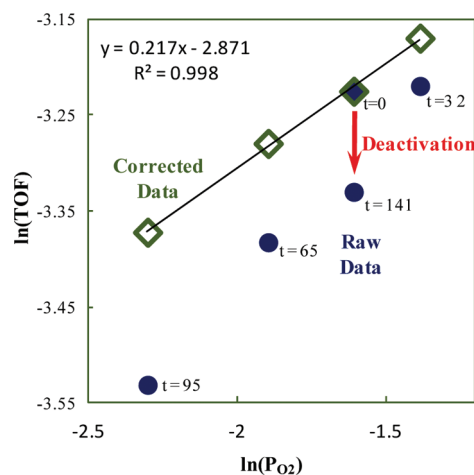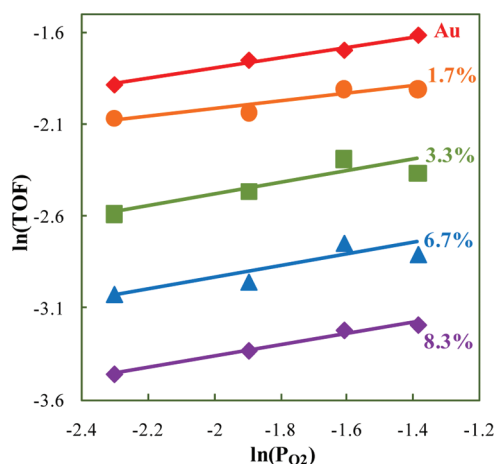
O_2 reaction order for each catalyst (top data set in Figure 4). Control experiments at constant O_2 pressure and with the unpoisoned catalyst showed that this treatment removed any systematic errors in the O_2 dependence studies and that any errors it introduced (<5%) were smaller than the inherent measurement errors in the reaction rate. This correction was therefore applied to all O_2 dependence studies to ensure consistency in the data. Oxygen reaction order data for the poisoned catalysts are presented in Figure 5 and compiled in Table 1. The data show little change in the reaction order as NaBr is added to the catalyst.

The oxygen pressure data can also be evaluated with double reciprocal plots (Figure 6) using a Michaelis–Menten type treatment.[25] This treatment is used to provide a means of extracting quantitative parameters that describe O_2 reactivity for individual gold catalysts; it is not intended to capture all of the molecular complexity of every elementary step in the reaction mechanism. A full derivation of this treatment has been previously published.[25] Briefly, a simple characterization

Table 1. Catalytic Activity Data for NaBr Poisoned Au Catalysts

mol % Br	rate[a] $(1/s)$	E_{app} (kJ/mol)	O_2 rxn order	ν_{max} $(1/s)$	K_R (atm)
0.0%	0.18	31.1	0.28	0.21	0.04
0.8%	0.16	31.3	0.31	0.20	0.06
1.7%	0.14	31.5	0.21	0.16	0.03
3.3%	0.11	31.8	0.27	0.14	0.06
5.0%	0.088	31.5	0.33	0.10	0.04
6.7%	0.065	30.3	0.33	0.09	0.07
8.3%	0.040	26.3	0.29	0.05	0.06
10%	0.017	35.0	0.24	0.03	0.04
12%	0.005	26.7	n.d.	n.d.	n.d.

[a]Reaction Conditions: 0 °C, P(O$_2$) = 0.2 atm, average of 2 runs on 2 different samples
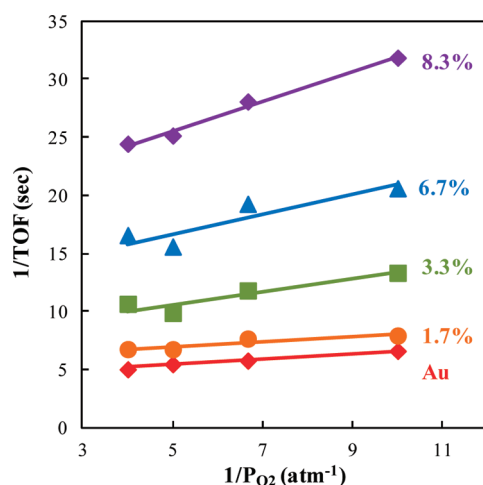
Figure 6. Double reciprocal plots for CO oxidation over NaBr poisoned Au/TiO$_2$ catalysts.

Scheme 1.
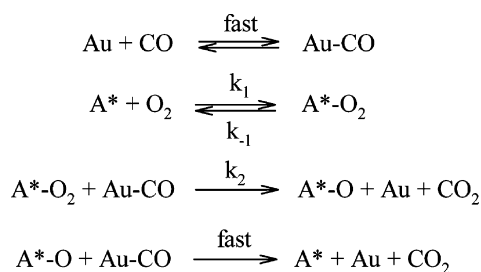
mechanism (Scheme 1), which has also been suggested by DFT calculations,[35,36] is used to describe the reaction.

The characterization mechanism in Scheme 1 is intentionally broad regarding the nature of the active site. Structurally, it only requires that O$_2$ is bound and activated someplace on the catalyst close to an Au surface atom capable of binding CO. Beyond this assumption, the characterization mechanism requires no further assumptions regarding the nature or structure of the active site. This assumption is widely agreed upon in the literature, although debate remains regarding the nature and structure of the active site (vide infra).[1,2] One of the goals of this work is to glean some insight into the number of active sites and possibly their nature; it is therefore prudent to make as few structural and kinetic assumptions as possible regarding the active site.

In the key kinetic steps of the characterization mechanism, oxygen is bound at an active site (A*) and then reacts with readily available CO to produce CO$_2$. Subsequent steps to produce a second equivalent of CO$_2$ and regenerate the active site are considered fast steps after the rate determining step and are therefore kinetically unobservable. Similarly, this mechanism is not intended to include the details of oxygen activation, as many reasonable possibilities exist (e.g., oxygen migration, O−O bond scission, O atom transfer to CO, etc.) for the actual rate determining step. The characterization mechanism is therefore an intentionally reductionist approach designed to help foster the extraction of chemically meaningful reaction metrics. It is not intended to advance specific mechanistic possibilities or make a priori assumptions regarding the nature of the active site.

Applying a typical kinetic derivation employing the steady-state approximation yields the following expression:

$$\frac{1}{\nu_{rxn}} = \frac{K_R}{\nu_{max}}\left(\frac{1}{P_{O_2}}\right) + \frac{1}{\nu_{max}} \tag{2}$$

where ν_{rxn} is the measured reaction rate and

$$\nu_{max} = k_2\theta_{CO}[A^*]_T \tag{3}$$

and

$$K_R = \frac{k_{-1} + k_2\theta_{CO}}{k_1} \tag{4}$$

We note that a similar set of equations can be derived using a Langmuir−Hinschelwood mechanism, although this requires some additional assumptions.[25] In these equations, θ_{CO} designates the coverage of the CO binding sites, which are a subset of the total Au surface sites, and $[A^*]_T$ is the total number of active sites. The total number of active sites is also assumed to involve a subset of the total number of surface Au sites. K_R and ν_{max} are descriptive kinetic parameters comparable to those employed in enzyme kinetics.[37] Analogous to the Michaelis−Menten constant, K_R is a measure of the reactivity or instability of adsorbed O$_2$ (cf. A*-O$_2$). Similarly, ν_{max} depends both on the intrinsic reaction barrier and the number of active sites. This kinetic treatment has been previously published and has been shown to describe well kinetic data for CO oxidation over several Au and bimetallic NiAu catalysts.[25,33]

The double reciprocal plots are generally quite linear, indicating that the Michaelis−Menten model is appropriate for this system. The extracted kinetic parameters K_R and ν_{max} are plotted against NaBr content in Figure 7. The data show a linear decrease in ν_{max} with added NaBr, with an x-intercept at 11.2% NaBr. This value is in excellent agreement with the TOF data shown in Figure 3. Additionally, there is little to no change in the K_R values for the catalysts: all are approximately 0.05 atm. For comparison, K_R increased by a factor of 40 when Ni was incorporated into Au nanoparticle catalysts.[33] The K_R data therefore provide no indication that NaBr addition affects oxygen activation.

DFT Calculations. DFT was used to gain further insight into how NaBr might poison the catalyst surface. Au clusters of any size will have a certain number of terrace, step, and other undercoordinated sites. As the particle size decreases, the ratio of these sites will change and the number of undercoordinated sites increases. The chosen model systems, Au(111), Au(211), and Au(532) are computationally easy to implement and have
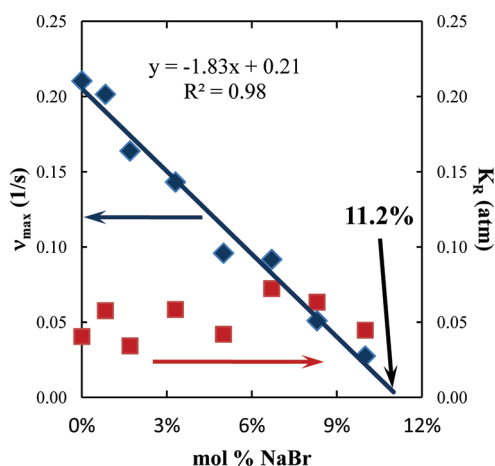
Figure 7. Kinetic parameters extracted from double reciprocal plots for CO oxidation over NaBr poisoned Au/TiO$_2$ catalysts. The x-axis refers to mol NaBr/total mol Au in the catalyst.

coordination numbers of 9, 7, and 6, respectively. Adsorption energies for O, CO, Br, and NaBr interacting with Au(111), Au(211), and Au(532) surfaces are reported in Table 2.

Table 2 shows that all adsorbates bind more strongly to the stepped (Au(211)) and kinked (Au(532)) sites than to the closed-packed (111) facet. Binding to the least coordinated surface (Au(532)) was found to be strongest for all the adsorbates, and calculated adsorption geometries for this surface are shown in Figure 8. Additionally, the adsorption energies for Br and NaBr on rutile TiO$_2$(110) were calculated to be 0.95 eV and −1.31 eV, respectively. The computational studies therefore indicate that NaBr adsorption onto the corner and edge atoms of supported Au nanoparticles is preferential to adsorption onto face atoms or the titania support.

This preference for low-coordinate atoms has been previously observed for CO and O adsorption on Au, and the calculated binding energy changes have been directly correlated to the coordination number of the most exposed Au surface atom.[38] More recently, it was shown that the CO and O binding energies are inversely proportional to the coordination number not only for Au, but also for a wide range of other transition metals.[39] Our results extend these previous findings and show that the same trend applies to Br and NaBr. The active sites for CO oxidation over Au nanoparticles have been suggested to be under-coordinated corner and edge sites,[40,41] so the preferential binding of bromide to these sites in silico and the experimentally observed bromide poisoning are consistent with these models.

Infrared Spectroscopy of Adsorbed CO. Infrared spectroscopy was used to further evaluate how NaBr addition might affect the catalyst surface. Figure 9 shows a representative experiment on the 5.0% NaBr poisoned catalyst. Details of the data analysis can be found in a separate publication.[27] Briefly,
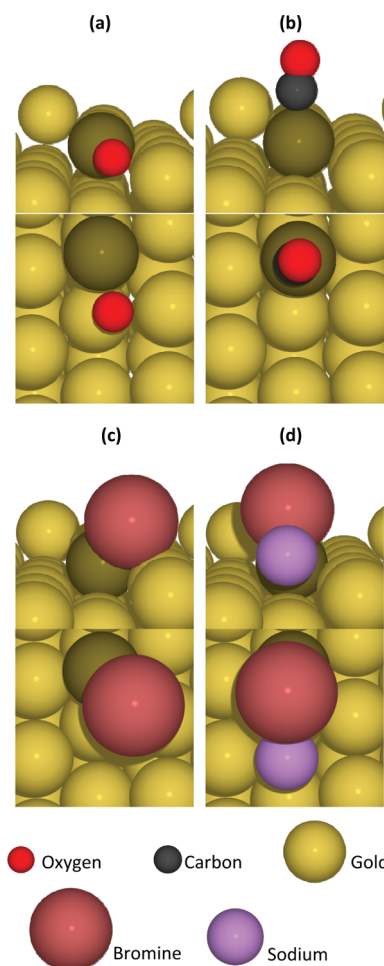

Figure 8. Binding geometries of (a) O, (b) CO, (c) Br, and (d) NaBr on the kinked Au(532) surface (split side and top views shown). The surface kink atom is colored darker for clarity.

the peak areas for the collected spectra are adjusted for any observed gas-phase CO and the resulting corrected peak areas ($\lambda_{max} \approx 2120-2100$ cm^{-1}, assigned to CO adsorbed on Au^0) are used to determine the adsorption isotherm (Figure 9 inset).

The adsorption isotherms were then fit using the Temkin adsorbate interaction model.[27] The linear portion of the data (usually corresponding to surface coverages between $\theta = 0.2-$ 0.8) and a previously determined ΔS_{ads} value of −142 J/(mol K) were used to extract two values that describe each catalyst.[27] The heat of adsorption at zero coverage (ΔH_0), which is determined from the y-intercept of the linear data, describes the nascent binding energy for CO on the catalyst when no adsorbate interactions are present. The second value, $\delta\Delta H$, describes the change in the adsorption energy from $\theta = 0$ to $\theta = 1$ (i.e., ΔH_0 to ΔH_1) with full coverage representing saturation of the CO binding sites, which is some subset of the total

Table 2. Calculated Adsorption Energies (in eV) of O, CO, Br, and NaBr on the Au(111), Au(211), and Au(532) Surfaces[a]

	O		CO		Br		NaBr	
Au(111)	fcc	0.29	top	−0.01	fcc	−0.65	fcc	−0.26
Au(211)	bridge	0.20	top	−0.30	bridge	−1.08	bridge	−1.29
Au(532)	kink	0.18	kink	−0.51	kink	−1.08	kink	−1.49
TiO$_2$(110)						0.95		−0.81

[a]Energies are reported in eV, referenced to O$_2$(g), CO(g), Br$_2$(g), and NaBr(g), respectively.
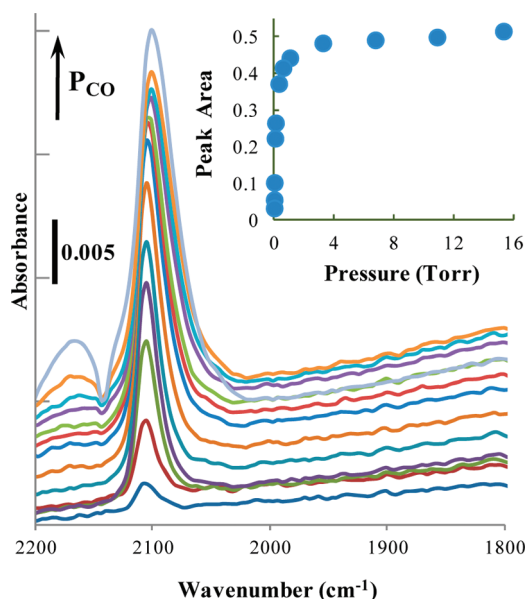
Figure 9. Infrared spectroscopy study of CO adsorbed on the 5.0% NaBr poisoned Au/TiO$_2$ catalyst at 0 °C. In this experiment, the pressure was varied incrementally from 0.003 (bottom spectrum) to 19.9 (top spectrum) Torr. The inset shows the adsorption isotherm for the experiment.
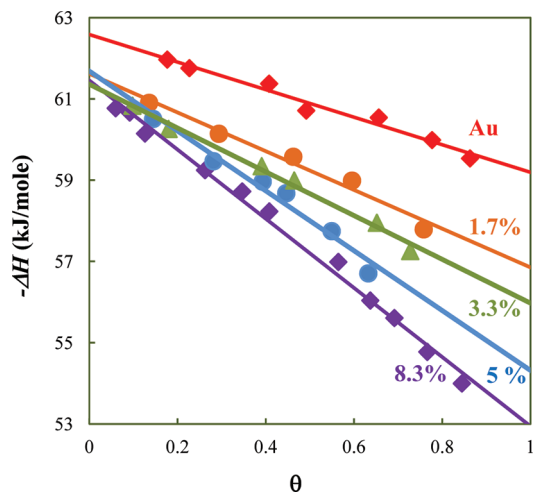

Figure 10. Temkin plots using the adsorbate interaction model for NaBr poisoned Au/TiO$_2$ catalysts.

number of surface Au sites. In the Temkin adsorbate interaction model, this change is attributed to electronic interactions between the CO adsorbates and the Au nanoparticles, and thus describes how the surface electronics change with coverage.[27]

Representative Temkin plots for the poisoned catalysts are shown in Figure 10; the extracted ΔH_0 and $\delta \Delta H$ values are plotted in Figure 11 and compiled in Table 3. The data suggest that the addition of NaBr may cause a slight decrease in ΔH_0, from about −63 kJ/mol to about −62 kJ/mol. This change appears to be largely independent of the amount of NaBr added, although it should be noted that the standard deviation for each measurement is about 0.7 kJ/mol, so this difference may not be statistically significant. The $\delta \Delta H$ term, on the other hand, more than doubles as NaBr is added to the catalyst, indicating NaBr affects the interactions between other
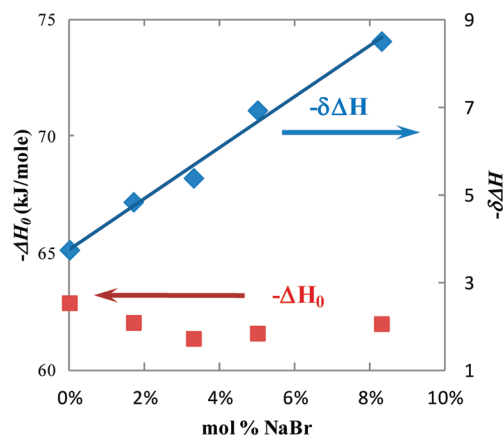

Figure 11. Extracted ΔH_0 and $\delta \Delta H$ values for NaBr poisoned Au/TiO$_2$ catalysts. The ΔH_0 values correspond to zero coverage; the $\delta \Delta H$ values describe the change in adsorption enthalpy from $\theta = 0$ to $\theta = 1$.

Table 3. Heat of Adsorption Values^a for CO on NaBr Poisoned Au/TiO$_2$ Catalysts

mol % Br	$-\Delta H_0$ (kJ/mol)	$-\Delta H_1$ (kJ/mol)	$-\delta \Delta H$ (kJ/mol)	θ_{CO} @ 7.6 Torr^b
0.0%	62.8 ± 0.3	59.1	3.7 ± 0.3	0.99
1.7%	62.0 ± 0.4	57.2	4.8 ± 0.1	0.97
3.3%	61.4 ± 0.1	56.0	5.4 ± 0.1	0.96
5.0%	61.8 ± 0.1	54.2	7.6 ± 0.4	0.92
8.3%	62.1 ± 0.5	53.4	8.7 ± 0.1	0.90

^{a}Adsorption isotherms measured at 0 °C from 0−20 Torr CO. Reported values are the average of 2 isotherm experiments. Reported errors are the range of experimental data. $^b\theta_{CO}$ values were calculated at 7.6 Torr CO and 273 K from the ΔH_0 and $\delta \Delta H$ data. The θ_{CO} value represents the coverage of the remaining (unpoisoned) CO binding sites.

adsorbates and the Au surface. As Figure 11 shows, this effect is proportional to the amount of NaBr added.

The extracted ΔH values can be used to calculate the CO coverage (θ_{CO}) under typical reaction conditions (7.6 Torr CO) for each catalyst.[27] Table 3 shows that θ_{CO} drops by only 10% for the 8.3% NaBr catalyst. It is important to clarify that the coverage for each catalyst is not an absolute surface coverage. In each case, the coverage term refers to the occupation of the available CO adsorption sites. Thus, any sites that might be blocked by adsorbed NaBr are not considered in this calculation, as they are not detected in the CO adsorption experiment. For comparison purposes, the catalytic activity for the 8.3% NaBr catalyst is more than 75% lower than for the pure Au/TiO$_2$ catalyst. Consequently, the changes in the θ_{CO} term are not likely to be a determining factor in the catalyst poisoning. To be clear, this refers to the relative coverage of *available* CO binding sites for a given catalyst. The absolute CO coverage likely decreases with added NaBr since NaBr binds more strongly to the corner and edge atoms than does CO (vide infra).

■ DISCUSSION

This study has two primary purposes: to understand and characterize the nature of halide poisoning on Au CO oxidation catalysts and to evaluate the number and type of active sites in these materials. Intentional poisoning experiments are particularly useful in exploring these issues as they provide a direct evaluation of the distribution of reactivities of various active

sites on the catalyst, and can help to discriminate between different poisoning mechanisms. Additionally, poisoning experiments provide a direct measure of the number of active sites on a catalyst, albeit a measure that remains open to interpretation. Intentional poisoning experiments have not been widely used in the literature, and we are aware of only a few studies where researchers have intentionally added a poison in a direct attempt to evaluate the number of active sites on a catalyst.[21] Finke[22] and Buriak[23] used CS_2 poisoning to examine supported Rh and Pt catalysts, respectively. Kung and co-workers recently examined bromide poisoning on Au/TiO_2 catalysts, although their study did not include the detailed kinetics, IR spectroscopy, or computational experiments presented here.[24] Kim and Woo also found that SO_2 addition poisons Au catalysts by generating surface sulfates, but they did not attempt to quantify this effect in terms of the number or type of active sites.[27]

Nature of the Poisoning. A key question in the application of intentional poisoning experiments is the nature of the poisoning. Poisoning can be due to strong interactions that prevent reactant molecules from accessing the catalytic active site (hereafter termed "site-blocking") or due to binding away from the active site that deleteriously affects the surface electronics required for catalysis to occur (hereafter described as an off-site or "electronic" poisoning mechanism, in which the poison binds away from the active site yet still modifies reactivity through some longer-range surface structural or electronic restructuring). As Finke and co-workers point out, site-blocking effects are generally local and can be minimized to the binding environment provided that a sterically small poison is used.[22] Electronic perturbations to the surface, on the other hand, may be long-range in nature and have been invoked to rationalize unusual poison/metal atom ratios.[22]

Beyond poisoning the catalysts and correlating activity loss with the amount of added poison, we evaluated the relative contributions of electronic and site-blocking mechanisms by adding detailed kinetic analyses of the poisoned catalysts and quantitatively evaluating CO adsorption with infrared spectroscopy. The kinetics and thermodynamics data are all consistent with a site blocking mechanism being the predominant mode of poisoning in this system. First, there is a linear decrease in catalyst activity with added NaBr. Two measures of activity were employed here, one under standard reaction conditions (TOF measured with 20% O_2) and one using all of the oxygen dependence data (kinetics model with ν_{max} parameter). Both data sets showed linear decreases in activity with added NaBr and had the same x-intercept (equivalents of NaBr required for 0 activity) at about 11 mol % NaBr. All the kinetics measurements were made under differential reaction conditions where reaction rates could be accurately determined from conversions. Second, as the catalyst activity dropped, there were essentially no changes in the other kinetic parameters that describe the system: the apparent activation energy (E_a), the O_2 reaction order, and K_R all showed no trends as NaBr was added to the catalyst. Third, the nascent heat of adsorption (ΔH_0) for CO on the catalyst was unaffected by the addition of NaBr. These data all indicate that the catalyst activity dropped without fundamentally changing the reaction mechanism or substantially altering the rate constants and heat of adsorption values for the species involved.

The changes in the Michaelis−Menten parameters are particularly compelling, as they employ the largest data sets (O_2 reaction order studies), are derived from a specific mechanistic model, and have clear physico-chemical interpre-

tations. In this mechanistic model, K_R describes reactivity of bound O_2 while ν_{max} is affected by both the O_2 reactivity and the total number of active sites. The K_R value varies by about a factor of 2 over all the catalysts studied, but there is little or no consistent trend in the variations. Further, this variation is small relative to the changes in ν_{max} and relative to the changes that we have reported for other catalysts. For comparison, a recent study on a series of $NiAu/TiO_2$ bimetallic catalysts found a 40-fold increase in K_R values relative to pure Au/TiO_2. Therefore, the changes in K_R associated with NaBr addition are not considered to be significant, particularly since Figure 7 shows no discernible trend in the values.

This leads to a second important conclusion regarding Au/TiO_2 catalysts, namely, that the active sites all have essentially the same inherent reactivity. If there were substantial differences in the nascent reactivities of the active sites, we would expect to observe either a nonlinear change in overall activity (with the most active sites being poisoned first) and/or substantial changes in K_R with NaBr addition. Equation 3 shows that ν_{max} depends on both the rate constant for reaction between O_2 and CO and the number of active sites. Since the K_R value does not significantly change with NaBr addition, it is reasonable to conclude that the k_2 term also does not change. As shown below, the coverage of CO on CO binding sites undergoes only a small change (less than 10%); consequently, changes in ν_{max} can be attributed primarily to changes in the number of active sites on the catalyst as NaBr is added.

The kinetics data (K_R, ν_{max}, apparent E_a, and oxygen dependence) all indicate that NaBr poisoning occurs primarily through a site-blocking mechanism. Potential electronic influences should also be examined, however. Infrared spectroscopy of adsorbed CO showed that the nascent heat of adsorption, ΔH_0, showed only a very small change (on the order of the measurement error) when NaBr was added to the catalyst. Additionally, Oxford and co-workers performed Au XANES studies on NaBr poisoned Au/TiO_2 catalysts. They reported no changes in the Au XANES adsorption edge structure, suggesting no change in the reduced/ionic character of Au, and similarly concluded that there was no experimental evidence of altering the electronic structure of the surface.[24]

The only potential electronic effects observed in this study are associated with CO adsorption experiments, in which the $\delta\Delta H$ term shows a consistent change with added NaBr (Figure 11, Table 3). This is an interesting result, particularly in light of the fact that the ΔH_0 term showed little to no change with NaBr poisoning. In the Temkin model for CO adsorption that we have developed, the $\delta\Delta H$ term is associated with changes in the coverage dependent indirect adsorbate−adsorbate interactions.[27] In the particular case of supported Au catalysts, these interactions appear to be mediated by a modest electronic modification of the Au surface.[27] In this particular case, CO binding becomes weaker as coverage increases; this phenomenon is likely due to increasing electron density in the Au s-band with CO adsorption, which reduces the strength of the interaction for subsequent adsorbates at higher coverages. The data from the poisoned catalysts indicate that NaBr addition seems to enhance this effect, increasing the magnitude of the adsorbate−surface−adsorbate interactions, resulting in weaker CO binding with increased coverage relative to the pure Au catalyst.

This is a potentially important effect because the kinetics experiments were performed with 7.6 Torr CO; at 0 °C, this results in coverage of the CO binding sites approaching unity.

To ensure that this was not affecting our interpretation, we calculated the coverage of CO binding sites under reaction conditions from the IR data (ΔH_0 and $\delta\Delta H$). As Table 3 shows, the CO binding site coverage drops by about 10% as NaBr is added. This does not appear to be an important effect in this system, particularly considering that Au binds CO much more strongly than O_2 and that the reaction operates in a zero-order kinetic regime with respect to CO. However, the IR data clearly show that NaBr addition does impact the catalyst electronics, albeit subtly. It is difficult to imagine how adsorption of a strong poison would have absolutely no effect on a catalyst, so the observation of at least a small electronic effect lends credence to the validity of the other studies. It also suggests that these IR measurements are extremely sensitive tests for examining catalyst electronics. We expect to pursue this more fully in future studies.

Nature and Number of Active Sites. Determining the number and nature of active sites is a key issue for all catalysts, and has been of particular interest for supported Au catalysts. A number of models for the active site in CO oxidation over supported Au catalysts have been offered.[1,14,19,42−48] For example, Yates, Neurock, and co-workers recently proposed that oxygen is activated through the formation of a CO-O_2 complex at the metal−support interface.[49] It is important to note that our Michaelis−Menten treatment makes very few assumptions regarding the nature of the catalytic active site, and is largely applicable to a number of potential active site structures. In fact, the only structural requirement in our kinetic derivation is that the active site for O_2 binding is close enough to a CO binding site to allow the two adsorbed species to react.

In the particular case of CO oxidation over Au/TiO$_2$ catalysts, assessing the number of active sites may help to describe the nature of the active sites. Chemisorption experiments often provide a measure of the number of surface atoms, and therefore a first estimate of the number of active sites; however, chemisorption experiments on supported Au catalysts are difficult, and have only been reported at very low temperature (e.g., −60 °C).[24,50,51] Particularly at low temperatures, these measurements are further complicated by physisorption on the high surface area titania support. Further, chemisorption experiments measure the number of surface atoms that bind a specific adsorbate; this may or may not be the same as the number of active sites on the catalyst. This is of particular concern for Au catalysts, where a number of suggestions for the CO oxidation active site have been posited.

Intentional poisoning experiments offer an additional means of evaluating the number of active sites because they directly track how activity changes with the added poison. As we have demonstrated above, NaBr poisoning of Au/TiO$_2$ catalysts is dominated by a site blocking mechanism. This simplifies quantitative interpretation of the poisoning experiments, as we do not need to consider potential electronic effects. Nonetheless, there are two critical issues that must be accounted for in evaluating the poisoning experiments as a kinetic titration for the number of active sites: (1) determining the location of the poison on the catalyst and (2) evaluating the stoichiometry between the poison and the active sites. Our computational study indicates that bromide has a strong preference for corner and edge atoms on Au NPs over face atoms. Bromide binding to a model titania support was calculated to be extremely weak. Similarly, a Br XANES study of NaBr poisoned Au/TiO$_2$ catalysts reported by Oxford and co-workers indicated that bromide was predominantly associated with Au.[24] These results

are consistent with the "softer" nature of bromide having a higher affinity for Au than for harder ions on the support (H$^+$, Ti^{4+}).[52] Consequently, it is reasonable to conclude that, at the levels introduced in this experiment, nearly all of the added NaBr interacts with the Au particles. This provides a very good first approximation to the number of active sites and deviations from this will result in a relatively small error from the actual value.

Issues with determining the poison to active site stoichiometry are more complicated; indeed, Finke and co-workers describe them as the "Achilles heel" of the method.[22] There are three general possibilities, which we will address below: (1) each deposited poison molecule blocks one active site, (2) each poison blocks more than one active site, and (3) more than one poison is required to block an active site. The first example is the most straightforward and provides a reasonable starting point for assessing the number of active sites on the catalyst. Under this scenario, the x-intercept in Figures 3 and 7 corresponds to the equivalents of poison required to eliminate catalytic activity, and therefore the number of active sites. On this basis, approximately 11% of the total Au is active for the reaction.

We have previously used TEM to determine an average particle size of 3.2 nm,[25] corresponding to a dispersion of 35−40%. Consequently, roughly 30% of the surface atoms are active for the reaction, assuming that each added NaBr poisons exactly one Au site. This value corresponds well with the expected fraction of low coordinate (CN = 6−7) corner and edge atoms (25−30% of surface atoms) expected for particles of this size.[53,54] This value carries the implicit assumption that all of the NaBr added is deposited on the Au nanoparticles, which is reasonable based on the present computational results and Oxford's XAS study.[24] The samples prepared were too small and had too little NaBr to determine Br content by elemental analysis or inductively coupled plasma atomic emission spectroscopy (ICP-AES). Given that these are qualitative comparisons, any errors introduced by bromide loss to glassware, adsorption on the support, and so forth are likely to be small.

A second possibility is that each poison blocks more than one active site. This would most commonly be associated with the poison bridging between two or more active atoms. However, the x-intercepts of the inhibition studies match up extremely well with the total number of corner and edge atoms, and the computational results indicate much weaker binding to coordinatively saturated face atoms. For this scenario to be at work here, CO or O_2 binding to highly coordinated face atoms in the reaction mechanism would need to be invoked. This seems unlikely for the particular case of CO oxidation over Au/TiO$_2$ catalysts. It is also possible that an adsorbate can restructure the surface, resulting in a change in the number of active sites. In this particular case, the computational studies indicate that bromide binds much more strongly to low coordinate atoms, which are inherently more energetic than face atoms. Therefore, there should be only a minimal thermodynamic driving force for the surface to restructure upon bromide adsorption to create a greater number of corner and edge atoms. Even if this does occur, it seems unlikely that the total number of corner and edge atoms would increase substantially because of NaBr addition.

A third possibility is that more than one poison is required to shut down an active site or that the number of active sites is a subset of sites that the poison binds. Unfortunately, this is very

difficult to differentiate from the case where each bromide poisons one active site. It is possible that some subset of the corner and edge atoms (for example, those near the metal–support interface) are responsible for the catalytic activity. Should any of these atoms be electron deficient due to interactions with the support, however, one would expect those electron deficient atoms to preferentially bind bromide relative to corner and edge atoms that are, by comparison, electron rich. Because the data in Figures 3 and 7 are linear, the bromide poisoning data show no evidence of a distribution of active sites or preferential binding. Further, the data correlate with the total number of corner and edge atoms, not with the number expected at or near the metal–support interface. Although this study cannot rule out the possibility that a subset of corner and edge atoms are the active sites for CO oxidation, there is also nothing in the data that points to such a scenario.

■ CONCLUSIONS

A commercial Au/TiO_2 catalyst was intentionally poisoned with NaBr to better understand the nature of halide poisoning of Au catalysts and to investigate the number and nature of the catalytic active sites. Catalytic testing of the poisoned catalysts showed a linear decrease in catalytic activity with added NaBr. This decrease in rate occurs with little to no change in key kinetic parameters such as the apparent activation energy, O_2 reaction order, or Michaelis–Menten type oxygen activation parameter (K_R). DFT calculations indicated that bromide preferentially adsorbs to Au surfaces over the titania support and that corner and edge atoms bind bromide more strongly than more highly coordinated face atoms. Infrared spectroscopy of adsorbed CO suggested that NaBr addition induces some subtle changes in the coverage dependent properties of CO adsorption, but these changes did not substantially impact the CO coverage of the CO binding sites. In total, these results indicate that halide poisoning for this system occurs primarily through a site-blocking mechanism. Further, the poisoning experiments suggest that 11% of the total Au, equivalent to about 30% of the surface Au, is active for the reaction. This value correlates well with the total number of corner and edge atoms expected for the catalyst.

■ AUTHOR INFORMATION

Corresponding Author
*E-mail: Bert.chandler@trinity.edu. Phone: (210) 999-7557. Fax: (210) 999-7569.

Notes
The authors declare no competing financial interest.

■ REFERENCES

(1) Bond, G. C.; Louis, C.; Thompson, D. T. *Catalysis by Gold*; Imperial College Press: London, U.K., 2006; Vol. 6.
(2) Kung, M. C.; Davis, R. J.; Kung, H. H. *J. Phys. Chem. C* **2007**, *111*, 11767.
(3) Corma, A.; Garcia, H. *Chem. Soc. Rev.* **2008**, *37*, 2096.
(4) Hashmi, S. K.; Hutchings Graham, J. *Angew. Chem., Int. Ed.* **2006**, *45*, 7896.
(5) Williams, W. D.; Shekhar, M.; Lee, W.-S.; Kispersky, V.; Delgass, W. N.; Ribeiro, F. H.; Kim, S. M.; Stach, E. A.; Miller, J. T.; Allard, L. F. *J. Am. Chem. Soc.* **2010**, *132*, 14018.
(6) Boucher, M. B.; Goergen, S.; Yi, N.; Flytzani-Stephanopoulos, M. *Phys. Chem. Chem. Phys.* **2011**, *13*, 2517.
(7) Deng, W.; Carpenter, C.; Yi, N.; Flytzani-Stephanopoulos, M. *Top. Catal.* **2007**, *44*, 199.
(8) Hutchings, G. J. *J. Catal.* **1985**, *96*, 292.
(9) Teles, J. H.; Brode, S.; Chabanas, M. *Angew. Chem., Int. Ed.* **1998**, *37*, 1415.
(10) Corma, A.; Serna, P. *Science (Washington, DC, U. S.)* **2006**, *313*, 332.
(11) Prati, L.; Rossi, M. *J. Catal.* **1998**, *176*, 552.
(12) Abad, A.; Concepcion, P.; Corma, A.; Garcia, H. *Angew. Chem., Int. Ed.* **2005**, *44*, 4066.
(13) Landon, P.; Collier, P. J.; Papworth, A. J.; Kiely, C. J.; Hutchings, G. J. *Chem. Commun. (Cambridge, U. K.)* **2002**, 2058.
(14) Chen, M. S.; Goodman, D. W. *Science (Washington, DC, United States)* **2004**, *306*, 252.
(15) Stiehl, J. D.; Kim, T. S.; McClure, S. M.; Mullins, C. B. *J. Am. Chem. Soc.* **2004**, *126*, 13574.
(16) Matthey, D.; Wang, J. G.; Wendt, S.; Matthiesen, J.; Schaub, R.; Laegsgaard, E.; Hammer, B.; Besenbacher, F. *Science (Washington, DC, United States)* **2007**, *315*, 1692.
(17) Janssens, T. V. W.; Clausen, B. S.; Hvolbaek, B.; Falsig, H.; Christensen, C. H.; Bligaard, T.; Norskov, J. K. *Top. Catal.* **2007**, *44*, 15.
(18) Comotti, M.; Li, W.-C.; Spliethoff, B.; Schueth, F. *J. Am. Chem. Soc.* **2006**, *128*, 917.
(19) Ganesh, P.; Kent, P. R. C.; Veith, G. M. *J. Phys. Chem. Lett.* **2011**, *2*, 2918.
(20) Oh, H.-S.; Yang, J. H.; Costello, C. K.; Wang, Y. M.; Bare, S. R.; Kung, H. H.; Kung, M. C. *J. Catal.* **2002**, *210*, 375.
(21) Gonzalez-Tejuca, L.; Aika, K.; Namba, S.; Turkevich, J. *J. Phys. Chem.* **1977**, *81*, 1399.
(22) Hornstein, B. J.; Aiken, J. D. III; Finke, R. G. *Inorg. Chem.* **2002**, *41*, 1625.
(23) Dehm, N. A.; Zhang, X.; Buriak, J. M. *Inorg. Chem.* **2010**, *49*, 2706.
(24) Oxford, S. M.; Henao, J. D.; Yang, J. H.; Kung, M. C.; Kung, H. H. *Appl. Catal., A* **2008**, *339*, 180.
(25) Long, C. G.; Gilbertson, J. D.; Vijayaraghavan, G.; Stevenson, K. J.; Pursell, C. J.; Chandler, B. D. *J. Am. Chem. Soc.* **2008**, *130*, 10103.
(26) Hartshorn, H.; Pursell, C. J.; Chandler, B. D. *J. Phys. Chem. C* **2009**, *113*, 10718.
(27) Pursell, C. J.; Hartshorn, H.; Ward, T.; Chandler, B. D.; Boccuzzi, F. *J. Phys. Chem. C* **2011**, *115*, 23880.
(28) Mortensen, J.; Hansen, L.; Jacobsen, K. *Phys. Rev. B* **2005**, *71*, 1.
(29) Enkovaara, J.; Rostgaard, C.; Mortensen, J. J.; Chen, J.; Dułak, M.; Ferrighi, L.; Gavnholt, J.; Glinsvad, C.; Haikola, V.; Hansen, H. a.; Kristoffersen, H. H.; Kuisma, M.; Larsen, a. H.; Lehtovaara, L.; Ljungberg, M.; Lopez-Acevedo, O.; Moses, P. G.; Ojanen, J.; Olsen, T.; Petzold, V.; Romero, N. a.; Stausholm-Møller, J.; Strange, M.; Tritsaris, G. a.; Vanin, M.; Walter, M.; Hammer, B.; Häkkinen, H.; Madsen, G. K. H.; Nieminen, R. M.; Nørskov, J. K.; Puska, M.; Rantala, T. T.; Schiøtz, J.; Thygesen, K. S.; Jacobsen, K. W. *J. Phys.: Condens. Matter* **2010**, *22*, 253202.
(30) Bahn, S. R.; Jacobsen, K. W. *Comput. Sci. Eng.* **2002**, *4*, 56.
(31) Hammer, B.; Hansen, L.; Nørskov, J. *Phys. Rev. B* **1999**, *59*, 7413.
(32) Monkhorst, H. J.; Pack, J. D. *Phys. Rev. B* **1976**, *13*, 5188.
(33) Chandler, B. D.; Long, C. G.; Gilbertson, J. D.; Vijayaraghavan, G.; Stevenson, K. J.; Pursell, C. J. *J. Phys. Chem. C* **2010**, *114*, 11498.
(34) We made several attempts to measure volumetric CO chemisorption on the unpoisoned Au/TiO_2 catalyst at 0 °C, using a TiO_2 sample to measure the weak adsorption on the support. Unfortunately, weak adsorption on the TiO_2 support was much larger

than the adsorption on surface Au, making reliable interpretation of the data impossible.

(35) Falsig, H.; Hvolboek, B.; Kristensen, I. S.; Jiang, T.; Bligaard, T.; Christensen, C. H.; Norskov, J. K. *Angew. Chem., Int. Ed.* **2008**, *47*, 4835.

(36) Nørskov and coworkers have proposed a similar mechanism based on DFT calculations (Falsig, H.; Hvolboek, B.; Kristensen, I. S.; Jiang, T.; Bligaard, T.; Christensen, C. H.; Norskov, J. K. *Angew. Chem., Int. Ed.* **2008**, *47*, 4835). The primary difference between Scheme 1 and the DFT results is that the Scheme 1 assumes that the reaction between surface O atoms and adsorbed CO (the last step in the scheme) is fast. The DFT study found this last reaction step to be fast for Au catalysts and further found that direct reaction between surface bound O_2 and adsorbed CO was required to accurately describe Au catalysts.

(37) Our first paper deriving and employing the Michaelis−Menten treatment used K_I to describe O_2 reactivity. Based on various feedbacks, we have changed the name of the constant to K_R so that it is not confused with a constant designed to describe inhibition.

(38) Kleis, J.; Greeley, J.; Romero, N. A.; Morozov, V. A.; Falsig, H.; Larsen, A. H.; Lu, J.; Mortensen, J. J.; Dulak, M.; Thygesen, K. S.; Norskov, J. K.; Jacobsen, K. W. *Catal. Lett.* **2011**, *141*, 1067.

(39) Peterson, A. A.; Grabow, L. C.; Brennan, T. P.; Ooi, C.; Wu, D. M.; Li, C. W.; Kushwaha, A.; Medford, A. J.; Mbuga, F.; Li, L.; Nørskov, J. K. *Top. Catal.* **2012**, submitted for publication.

(40) Falsig, H.; Hvolboek, B.; Kristensen, I. S.; Jiang, T.; Bligaard, T.; Christensen, C. H.; Noerskov, J. K. *Angew. Chem., Int. Ed.* **2008**, *47*, 4835.

(41) Min, B. K.; Friend, C. M. *Chem. Rev. (Washington, DC, U. S.)* **2007**, *107*, 2709.

(42) Raphulu, M. C.; McPherson, J.; van, d. L. E.; Anderson, J. A.; Scurrell, M. S. *Gold Bull. (London, U. K.)* **2010**, *43*, 334.

(43) Tost, A.; Widmann, D.; Behm, R. J. *J. Catal.* **2009**, *266*, 299.

(44) Laursen, S.; Linic, S. *Phys. Chem. Chem. Phys.* **2009**, *11*, 11006.

(45) Rashkeev, S. N.; Lupini, A. R.; Overbury, S. H.; Pennycook, S. J.; Pantelides, S. T. *Phys. Rev. B: Condens. Matter Mater. Phys.* **2007**, *76*, 035438/1.

(46) Overbury, S. H.; Schwartz, V.; Mullins, D. R.; Yan, W.; Dai, S. *J. Catal.* **2006**, *241*, 56.

(47) Calla, J. T.; Davis, R. J. American Chemical Society: 2006; p COLL.

(48) Remediakis, I. N.; Lopez, N.; Norskov, J. K. *Angew. Chem., Int. Ed.* **2005**, *44*, 1824.

(49) Green, I. X.; Tang, W.; Neurock, M.; Yates, J. T. Jr. *Science (Washington, DC, U. S.)* **2011**, *333*, 736.

(50) Menegazzo, F.; Manzoli, M.; Chiorino, A.; Boccuzzi, F.; Tabakova, T.; Signoretto, M.; Pinna, F.; Pernicone, N. *J. Catal.* **2006**, *237*, 431.

(51) Menegazzo, F.; Pinna, F.; Signoretto, M.; Trevisan, V.; Boccuzzi, F.; Chiorino, A.; Manzoli, M. *Appl. Catal., A* **2009**, *356*, 31.

(52) Pearson, R. G. *J. Am. Chem. Soc.* **1963**, *85*, 3533.

(53) Van, H. R.; Hartog, F. *Surf. Sci.* **1969**, *15*, 189.

(54) Janssens, T. V. W.; Clausen, B. S.; Hvolbaek, B.; Falsig, H.; Christensen, C. H.; Bligaard, T.; Norskov, J. K. *Top. Catal.* **2007**, *44*, 15.